THE ASTRONOMICAL JOURNAL, 118:1444–1449, 1999 October

CTQ 414: A NEW GRAVITATIONAL LENS[1]

NICHOLAS D. MORGAN,[2] ALAN DRESSLER,[3] JOSÉ MAZA,[4,5] PAUL L. SCHECHTER,[2] AND JOSHUA N. WINN[2]

Received 1999 May 17; accepted 1999 June 8

ABSTRACT

We report the discovery and ground-based observations of the new gravitational lens CTQ 414. The source quasar lies at a redshift of $z = 1.29$ with a B magnitude of 17.6. Ground-based optical imaging reveals two point sources separated by 1.″2 with a magnitude difference of roughly 1 mag. Subtraction of two stellar point-spread functions from images obtained in subarcsecond seeing consistently leaves behind a faint, residual object. Fits for two point sources plus an extended object places the fainter object collinear with the two brighter components. Subsequent *Hubble Space Telescope* Near Infrared Camera and Multi-Object Spectrometer (NICMOS) observations have confirmed the identification of the fainter object as the lensing galaxy. Very Large Array observations at 8.46 GHz reveal that all components of the lensing system are radio-quiet down to the 0.2 mJy flux level.

Key words: gravitational lensing — quasars: individual (CTQ 414)

1. INTRODUCTION

Gravitational lensing is a powerful tool with a wide range of astrophysical applications (Kochanek & Hewitt 1996). In particular, multiply imaged quasars have become a useful probe for a number of cosmological investigations, such as measurements of the Hubble constant (Refsdal 1964) and statistical constraints on the cosmological constant (Kochanek 1996). The usefulness of gravitationally lensed quasars, however, is limited by the relatively few systems discovered to date. In this paper, we report our discovery and analysis of a new multiply imaged quasar.

CTQ 414 ($1^h58^m41\overset{s}{.}43$, $-43°25'3\overset{''}{.}4$, J2000.0) was originally identified as a $z = 1.29$, $B = 17.2$ quasar from the Calán-Tololo Survey (CTS; Maza et al. 1995), a survey designed to discover quasars and emission-line galaxies in the southern hemisphere. In 1997 August, optical observations of approximately 200 of the CTS quasars were carried out at the Cerro Tololo Inter-American Observatory (CTIO). The primary purpose of this effort was to determine if any of the selected CTS quasars exhibited evidence of arcsecond, multiple images that would arise from gravitational lensing. Prior to this run, another Calán-Tololo quasar, CTQ 286, had been found by Claeskens, Surdej, & Remy (1996) to be lensed. CCD exposures of CTQ 414 immediately revealed it to be double, with a separation of 1.″2 evident in B, V, R, and I filters.

We present the details of these observations, along with their subsequent analysis, in § 2. Also described in § 2 are follow-up observations conducted at the Las Campanas Observatory (LCO) 2 weeks later, as well as our photometric analysis of the lens components utilizing astrometric positions obtained from *Hubble Space Telescope* (*HST*)/Near Infrared Camera and Multi-Object Spectrometer (NICMOS) imaging. In § 3, we present our astrometric and photometric results for stars in the quasar field. In 1998 May, the Very Large Array (VLA) was used to search for radio counterparts of CTQ 414. We discuss these observations in § 4. Finally, in § 5, we summarize our findings for CTQ 414.

2. OPTICAL OBSERVATIONS AND ANALYSIS

2.1. *Initial Optical Imaging: Detection of System Duplicity*

Initial optical observations of CTQ 414 were obtained by one of us (P. L. S.) at CTIO between the nights of 1997 August 26–30. The 1.5 m telescope equipped with the Tektronix 2048 No. 6 CCD was used, although only the central 1536×1536 array was read out. The field of view of the camera was 6.2 arcmin^2 with a scale of 0.″2417 pixel^{-1}, a gain of 2 e^- ADU^{-1} (analog-to-digital unit), and a read noise of 5 e^-. A total of 20 exposures of CTQ 414 were obtained with Johnson BV and Kron-Cousins RI filters on the nights of August 26, 27, and 29. Each exposure lasted 300 s, and was obtained through air masses ranging from 1.027 to 1.143 over the course of the three nights. Seeing conditions ranged from 1.″16 to 1.″93 FWHM. Multiple 60 s $BVRI$ exposures of two Landolt photometric standard fields (fields PG 0231+051 and PG 2331+055) were also obtained during two of the above nights. Our exposures of PG 0231+051 and PG 2331+055 contained five and three Landolt standard stars, respectively. A log of the observations for CTQ 414 is presented in Table 1. Figure 1 shows an R-band exposure of CTQ 414 and the surrounding field obtained in 1.″25 FWHM seeing. The reader will note the relative absence of comparably bright stars in this high-latitude field.

Each CCD frame was bias-subtracted, trimmed, and flat-field–corrected using the VISTA reduction program. The flat-field images were cleaned of cosmic rays using AUTOCLEAN, a program written and kindly supplied by J. Tonry. As mentioned in § 1, images of CTQ 414 appeared double in all exposures (see Fig. 2*a*). We therefore fitted the double images with two empirical point-spread functions (PSFs), using a variant of the program DoPHOT

[1] Based on observations carried out at the Cerro Tololo Inter-American Observatory (CTIO), the Las Campanas Observatory (LCO), and the National Radio Astronomy Observatory (NRAO) Very Large Array (VLA). CTIO is part of the National Optical Astronomy Observatories, which are operated by the Association of Universities for Research in Astronomy, Inc., under cooperative agreement with the National Science Foundation. The NRAO is a facility of the National Science Foundation operated under cooperative agreement by Associated Universities, Inc.

[2] Department of Physics, Massachusetts Institute of Technology, Cambridge, MA 02139; ndmorgan@mit.edu, schech@achernar.mit.edu, jnwinn@mit.edu.

[3] Observatories of the Carnegie Institution of Washington, 813 Santa Barbara Street, Pasadena, CA 91101; dressler@ociw.edu.

[4] Departamento de Astronomía, Universidad de Chile, Casilla 36-D, Santiago, Chile; jmaza@das.uchile.cl.

[5] Cátedra Presidencial de Ciencias 1996–1998.

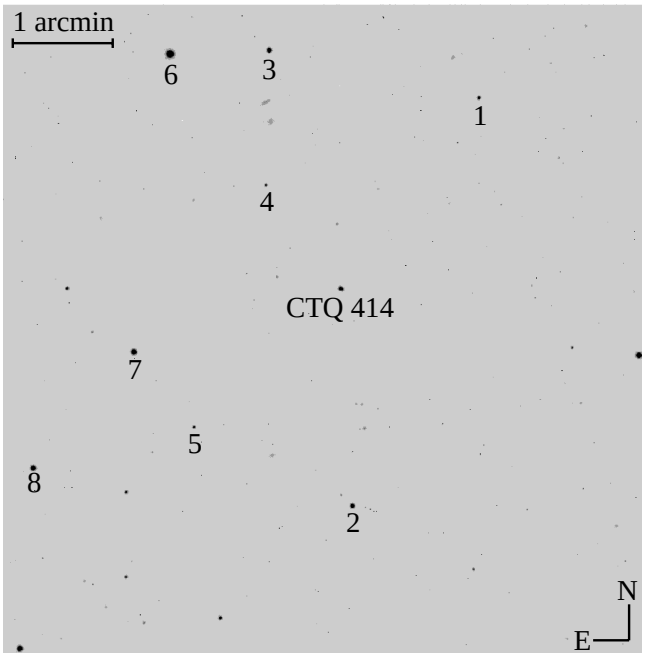

FIG. 1.—300 s *R*-band image of CTQ 414 and surrounding stars taken at CTIO. Photometric and astrometric results have been obtained for stars 1–8.

TABLE 1

LOG OF OBSERVATIONS FOR CTQ 414 AT CTIO

Frame	Filter	FWHM (arcsec)	Frame	Filter	FWHM (arcsec)
104.....	*R*	1.31	233.....	*R*	1.30
105.....	*B*	1.48	399.....	*R*	1.42
106.....	*V*	1.43	401.....	*R*	1.25
107.....	*B*	1.38	402.....	*B*	1.18
108.....	*I*	1.30	403.....	*V*	1.16
211.....	*R*	1.32	405.....	*I*	1.30
212.....	*B*	1.47	406.....	*I*	1.26
213.....	*V*	1.93	408.....	*I*	1.24
214.....	*V*	1.59	409.....	*B*	1.39
215.....	*I*	1.47	410.....	*V*	1.25

(Schechter, Mateo, & Saha 1993), designed to deal with close, pointlike, and extended objects (Schechter & Moore 1993). Star 7 in Figure 1 was used as the empirical PSF. These fits yielded average separation distance between the two components in *B*, *V*, *R*, and *I* of $1''.200 \pm 0''.006$, $1''.222 \pm 0''.012$, $1''.215 \pm 0''.009$, and $1''.193 \pm 0''.010$, respectively. We note that the smaller separation in *I*-band is consistent with the presence of a relatively red object between the double image. However, no consistent or suggestive pattern of residuals was found upon fitting and subtracting the two

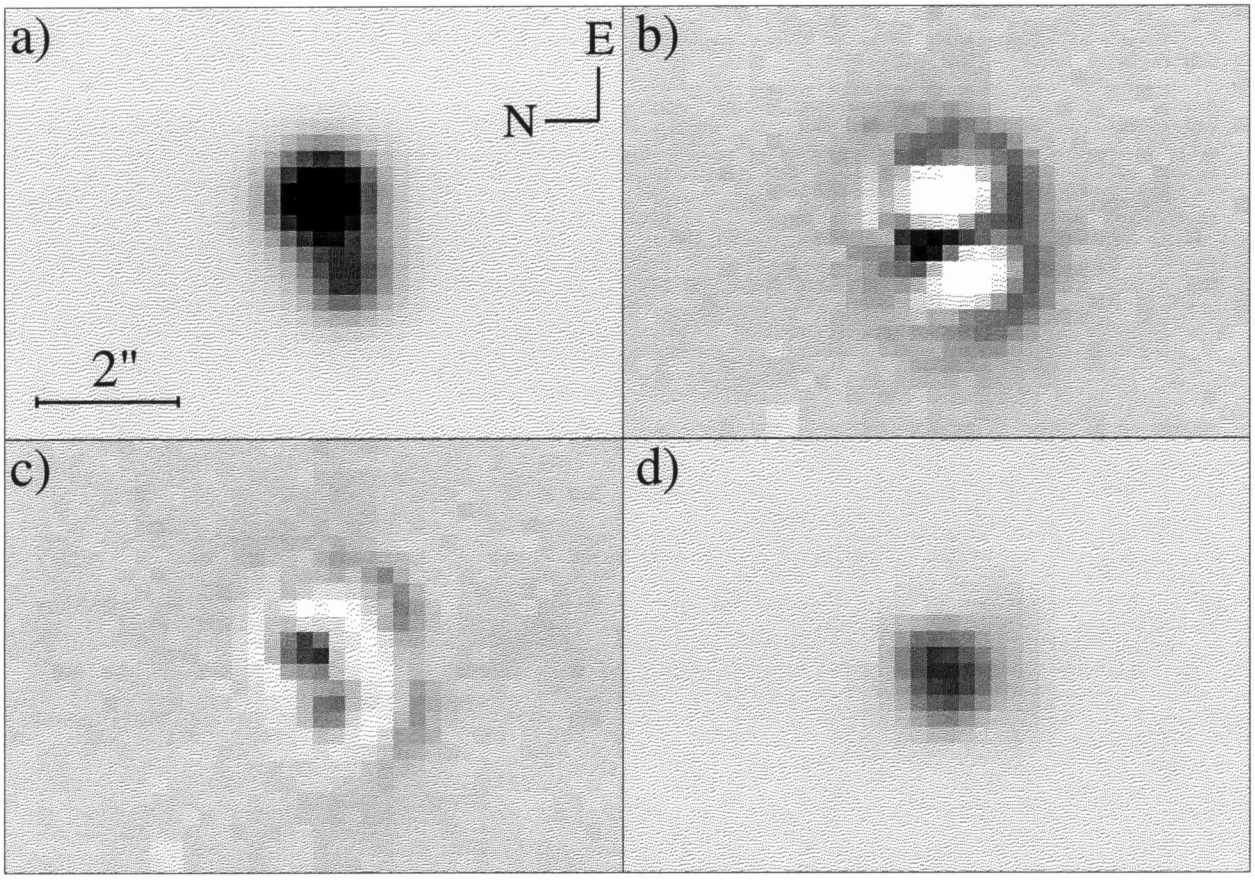

FIG. 2.—(*a*) Summed image of the 12 *R*-band exposures of CTQ 414 taken at LCO. The scale for the image is $0''.2278$ pixel^{-1}. East is at the top and north is to the left. The fainter component is at P.A. 251° east of north. (*b*) Summed image after fitting and subtracting two stellar PSFs from the individual frames. (*c*) Summed image after fitting and subtracting two stellar PSFs plus a pseudo-Gaussian from the individual frames. (*d*) Summed image after fitting and subtracting two stellar PSFs from the individual frames, but leaving the pseudo-Gaussian unsubtracted. Contrast in (*b*) and (*c*) is higher by a factor of 12 than in (*a*). Contrast in (*d*) is higher by a factor of 4 than in (*a*).

PSFs, although the difficulty of fitting for multiple point sources separated by less than a seeing disc should be noted.

2.2. *Follow-up Optical Imaging: Detection of a Third Object*

Following the initial imaging of CTQ 414 taken in 1997 August at CTIO, an additional 12 exposures were obtained by one of us (A. D.) at LCO on the night of 1997 September 10. The 2.5 m du Pont Telescope equipped with a Tektronix No. 2 CCD detector was used. The CCD camera has a field of view of 3.9 arcmin^2 with a scale of 0.″2278 pixel^{-1}. The camera was set in the No. 3 gain position, providing a gain of 3.9 e^- ADU^{-1} and a read noise of 9.4 e^-. Seeing for the night ranged from 0.″89 to 1.″08 FWHM, significantly better than the initial images from CTIO taken 2 weeks earlier. All 12 images were taken in *R* band and each exposure lasted 300 s.

The frames were bias-subtracted, trimmed, and flat-field–corrected, following the same procedure as mentioned above. Simultaneous fitting of two empirical PSFs (using the identical star as noted in the previous subsection) resulted in an average separation between the two components of 1.″198 $\pm$ 0.″001. This separation agrees well with the average *R*-band separation obtained from the CTIO data.

Subtraction of the two empirical PSFs produced a consistent pattern of residuals present in all 12 frames (see Fig. 2*b*). This pattern consisted of a bright spot located slightly west of component A and northeast of component B, as well as two crescent-like arcs of positive residuals to the southeast of each component, and two regions of negative "cavities" located at the centers of A and B. The amplitude of the bright spot is quite small, of order 2%–3% of the central intensity of component A. The crescent is 1%–2% of A's central intensity, while the cavities for A and B were 3%–4% and 2%–3% of A's central intensity, respectively.

One possible explanation for this pattern of residuals is that the fitting program is trying to account for three sources of light with just two point sources. If the unaccounted source of light were located between and displaced slightly to the northwest from the two components, then the PSFs would be dragged off-target from the centers of components A and B in an attempt to cover the extra light. This would produce the observed crescent pattern of residuals along the southeast edge. Also, the observed cavities would arise from attributing excessive flux to components A and B in an attempt to account for the three sources of light in the system.

Another possibility is that we are seeing an artifact of a poor PSF template. Such an effect might arise from variations in the PSF across the surface of the CCD, or from mistakenly using an extended object as our model point source. However, we do not believe that either of these explanations is correct, since the identical residual pattern persists even when different stars from across the face of the detector are used as our PSF.

Following the suggestive pattern of the residuals, we decided to fit each frame of the LCO data for two point sources plus an extended object (hereafter C), which we interpret here as the lensing galaxy. The object was modeled as a circularly symmetric pseudo-Gaussian as described in Schechter et al. (1993), convolved with the seeing conditions. The positions and fluxes of all three components, as well as the size σ of the pseudo-Gaussian, were treated as free parameters.

The averaged results for these fits placed component C collinear with components A and B and at an angular distance of 0.″72 $\pm$ 0.″03 away from A. The separation between components A and B was determined as 1.″29 $\pm$ 0.″02. Note that this solution for the lensing galaxy places it roughly midway between components A and B. The rms scatter in the galaxy position was 0.″034 along the North-South direction, and 0.″088 along the East-West direction, in both cases small compared with the relative distances between the three components. Flux ratios of components B to A and components C to A were 32.6% $\pm$ 0.6% and 20.5% $\pm$ 0.5%, respectively. The average σ of the pseudo-Gaussian used to model component C was found to be 0.″32 $\pm$ 0.″010.

This result for the position of the lensing galaxy, that it is very nearly equidistant from the two quasar images, would appear to be inconsistent with the unequal flux ratio of the two quasar components. For an isothermal lens, the flux ratio for the components would be proportional to the ratio of their distances from the lensing galaxy.

A very similar situation was encountered in the case of FBQ 0951+2635 (Schechter et al. 1998), with the position of the lensing galaxy too well centered for the unequal flux ratio. The parameters for the ground-based observations for this system were quite similar to those for CTQ 414. Subsequent imaging of FBQ 0951+2635 with *HST* NICMOS confirmed the presence of the lensing galaxy (B. A. McLeod et al. 1998, private communication) but placed it considerably closer to the fainter image than did the ground-based observations. A similar systematic error of this sort with CTQ 414 would not be surprising, given the difficulty of measuring a third object between two objects separated by only one seeing disk.

2.3. *Confirmation of the Lensing Galaxy*

In an attempt to confirm the lensing hypothesis, CTQ 414 was placed onto the CfA-Arizona Space Telescope Lens Survey (CASTLES; Kochanek et al. 1998) observing program at the suggestion of the authors. The suspected lens was imaged by *HST* NICMOS in four 640 s *H*-band exposures on 1998 August 4. These exposures clearly reveal the extended emission of the lensing galaxy, and place it approximately collinear with the two quasar images (E. E. Falco et al. 1998, private communication).[6] Gaussian fits for the positions of components B and C with respect to component A places B 1.″22 from A at P.A. 251.°0 east of north, and the nucleus of component C 0.″80 from A at P.A. 253.°4 east of north. As suspected, the true position of the lensing galaxy is $\sim$10% closer to the fainter quasar image than indicated by the ground-based data.

2.4. *Photometric Analysis of Lens Components*

Photometry of the lens components was performed using the same variant of DoPHOT described above. Photometric solutions to the LCO data set were obtained by fixing the relative separations of components A, B, and C at the corresponding *HST* positions. The fluxes of the three components, as well as the overall position of the system

[6] The *HST* images of CTQ 414 are available to download from the CASTLES ftp site or may be viewed on-line at the CASTLES home page at http://cfa-www.harvard.edu/glensdata.

and the size σ of the lensing galaxy, were treated as free parameters. In the process of fixing the relative separations of the system components, appropriate steps were taken to account for the plate scale and chip orientation of the LCO detector. Table 2 summarizes our photometric results for the LCO data set. Here we present the separate magnitudes of components A, B, and C, as well as magnitude differences between system components and the combined magnitude from the two quasar images.

A similar attempt was made to determine the colors of the lens components using the *BVRI* data from CTIO. Again, relative separations were fixed at the corresponding *HST* values, while the overall position of the system, the fluxes of components A, B, and C, and the size σ of the lensing galaxy were treated as free parameters. Appropriate steps were again taken to account for the plate scale and chip orientation of the CTIO detector. Unfortunately, treating the flux and size of component C as free parameters introduced too much freedom into these models, and the fits failed to converge to our satisfaction. Fixing the size σ of the lensing galaxy across all wavelengths at the LCO *R*-band value resulted in no noticeable improvement. The quality of seeing on the CTIO data set is simply not good enough to perform stable photometry of component C. Reliable colors of all three system components will require better images.

To circumvent this problem to some extent, we decided to set the flux of the lensing galaxy to zero and solve only for the fluxes of components A and B. Relative positions were still held constant at the corresponding *HST* values, while the overall position of the system was free to vary. Table 3 presents our magnitude results for the combined flux of components A and B. Admittedly, these results contain a systematic error by failing to take into account light from the lensing galaxy. Upon comparison with the corresponding LCO result presented in Table 2, we find that the combined CTIO A+B magnitude in *R* is brighter than the corresponding LCO result by 0.08 mag. Under the assumption that the lensing galaxy gets brighter in redder wavelengths, we would expect a correspondingly smaller systematic error in *B* and *V* bands and a larger one in *I*. It is hoped that these results will provide a handle on future variability of the system across *BVRI* wavelengths.

TABLE 2

PHOTOMETRIC SOLUTIONS FOR LCO DATA

	ΔR.A. (s)	Δdecl. (arcsec)	Δm_R	m_R
A	0	0	0	17.338 ± 0.001
B	−0.1061	−0.398	-1.149 ± 0.004	18.487 ± 0.004
C	−0.0700	−0.228	-2.102 ± 0.027	19.440 ± 0.028
A+B.....	...	...	...	17.018 ± 0.003

NOTE.—Relative positions for components A, B, and C were obtained from *HST* NICMOS imaging and were held fixed during our photometric solution. Error bars are from the observed dispersion between the images and do not include uncertainties in the magnitude of the PSF template star (see note to Table 5).

3. PHOTOMETRIC AND ASTROMETRIC STANDARDS

3.1. *Photometric Standards*

Photometric and astrometric results for stars in the CTQ 414 field were obtained for use with future observations. Eight nearby reference stars within a 4′ radius from the target lens were chosen for this purpose. These stars are identified by the labels shown in Figure 1.

Observations of the Landolt (1992) standard fields PG 0231+051 (PG 0231+051, PG 0231+051A, PG 0231+051B, PG 0231+051C, PG 0231+051D) and PG 2331+055 (PG 2331+055, PG 2331+055A, PG 2331+055B) were used to derive color terms and zero-point offsets for calibration onto the Johnson-Kron-Cousins photometric system. Table 4 lists the color terms used for the transformations as well as the number of standard stars *N* used and the corresponding rms scatter of the fit. Color terms were extracted from the PG 0231+051 field, using the field's greater sampling of $B-V$ indexes as compared to the PG 2331+055 field. Zero-point offsets were derived from the PG 2331+055 field. In deriving the *I*-band color term, the faintest of the five observed PG 0231+051 standard stars was discarded (see below). We have solved for the transformation equations in the form

$$X - x = \text{const} + a_1(B - V)\,, \quad (1)$$

$$B - V = \text{const} + a_2(b - v)\,, \quad (2)$$

where X represents the apparent magnitude in the standard *BVRI* system, x represents the extinction-corrected instrumental magnitude above Earth's atmosphere, and a_1 and a_2 represent the respective color terms for the $X - x$ and $B-V$ transformations. Corrections for atmospheric extinction were applied using "typical" extinction coefficients as cited in the 1990 CTIO Facilities Manual ($k_B = 0.22$, $k_V = 0.11$, $k_R = 0.08$, $k_I = 0.04$).

In the process of reducing the standard fields, the relatively faint star PG 0231+051 (with Landolt values $I = 16.64$ and $B-V = -0.33$) was discovered to be brighter in *I* by 0.30 ± 0.05 mag with respect to Landolt's (1992) listed magnitude. This residual is in the sense $I_{\rm stnd} - I_{\rm obs}$, in which $I_{\rm stnd}$ is the value reported by Landolt (1992) and $I_{\rm obs}$ has been computed from the transformations given above. Similar *I*-band discrepancies for PG 0231+051, as compared with the Landolt (1992) standard value, have been reported by Geisler (1996), who found an *I* residual of 0.23 mag, and also by Rosvick (1995), who found an *I* residual of 0.15 mag. The residual reported by Geisler is in the same sense as mentioned above, while Rosvick does not report the sense of his residual. Because of the observed discrepancy, the *I*-band observations of PG 0231+051 were not included in the solution of the *I*-band color term.

TABLE 3

PHOTOMETRIC SOLUTIONS FOR CTIO DATA

	B	*V*	*R*	*I*
$m_{\rm A+B}$.....	17.627 ± 0.004	17.334 ± 0.010	16.932 ± 0.007	16.728 ± 0.004

NOTE.—Source of error bars same as for Table 2; see note to Table 5.

TABLE 4

COLOR TERMS FOR TRANSFORMATION EQUATIONS

Index	N	a_1	a_2	rms
B	15	−0.0807	...	0.0099
V	10	0.0110	...	0.0244
R	10	−0.0194	...	0.0134
I	8	0.0363	...	0.0184
$B-V$	...	...	−0.0847	0.0218

The empirical PSF fitting described in the previous section yields magnitudes of stars in the quasar field with respect to the template PSF star. With the template star placed onto the standard photometric system, magnitudes for the field stars are straightforward to obtain. Apparent *BVRI* magnitudes for our eight reference stars are listed in Table 5, along with respective standard errors of the mean ($\sigma/N^{1/2}$) as derived from frame-to-frame scatter. These error bars do not include uncertainties in the reference star's calibration, which are listed in the note to Table 5. Object numbers in Table 5 correspond to the labels in Figure 1. These local standards were used to calibrate the LCO photometry results reported in Table 2.

It should be noted that images taken from CTIO are afflicted by coma aberration. The CTIO 1.5 m is a Ritchey-Chrétien telescope designed to operate free from coma aberration at an aspect-ratio of f/7.5, but not at f/13.5. Observations at CTIO were carried out at f/13.5 to use the smaller pixel scale at that f-ratio. The presence of coma aberration results in a slight, off-axis distortion in the PSF shape across the face of the detector. By comparing magnitudes derived from multiple PSF fitting, we estimate that coma aberration for our images is a small effect, introducing uncertainties in our magnitude determinations of 0.02 mag for stars on the largest contours of constant-wavefront aberration.

3.2. *Astrometric Standards*

Astrometric solutions were also obtained for the eight reference stars in the quasar field using one of the *R*-band exposures taken through a seeing of 1.″32 FWHM. This particular exposure was chosen since it yielded the lowest rms position errors with respect to standard coordinates. Standard coordinates for the objects were taken from the APM Sky Catalogue at Cambridge, England. The astrometric results are included in Table 5. The reported positions are in the form of offsets from star 7, in the sense of star x minus star 7.

4. RADIO OBSERVATIONS

On 1998 May 19 we searched for radio emission from CTQ 414, using the NRAO VLA. The search was carried out at 8.46 GHz, while the VLA was in the A configuration. This provided an east-west resolution of 0.″2. Our 14 minute observation bracketed the transit time of CTQ 414, at an altitude of 12°, permitting a north-south resolution of approximately 1″.

No significant sources of radio flux were detected within a 5″ error circle around the position of CTQ 414. The rms noise level in this field was 0.065 mJy per synthesized beam, so our observation rules out (at the 3 σ level) any sources of compact flux above 0.2 mJy. This is unfortunate but not particularly surprising, since the large majority of known quasars are radio-quiet.

5. SUMMARY AND CONCLUSIONS

We have reported our discovery and photometric analysis of the new gravitational lens CTQ 414. Ground-based optical images of the quasar appear double with a separation of 1.″2 and a magnitude difference between the quasar images of roughly 1 mag. Fitting and subtracting two empirical point-spread functions to images obtained in subarcsecond seeing consistently leaves behind a faint, residual object. Fits for two PSFs plus an extended object place the extended object collinear with the pair of brighter components. Subsequent *HST* imaging with NICMOS has indeed confirmed the extended object as the lensing galaxy. We have shown that ground-based photometric analysis of all three lens components is feasible with subarcsecond seeing conditions, and hope that the photometric analysis presented in this paper will provide a handle on any future variability of the quasar images.

N. D. M. and P. L. S. gratefully acknowledge the support of the U.S. National Science Foundation through grant AST 96-16866. J. N. W. thanks the Fannie and John Hertz Foundation for financial support. J. M. thanks FONDECYT, Chile, for support through grant 1980172.

TABLE 5

RELATIVE ASTROMETRY AND ABSOLUTE PHOTOMETRY FOR NEARBY REFERENCE STARS

Object	ΔR.A. (s)	Δdecl. (arcsec)	m_B	m_V	m_R	m_I
1	−18.255	149.32	19.563 ± 0.018	18.519 ± 0.023	17.987 ± 0.008	17.482 ± 0.025
2	−11.794	−87.49	19.462 ± 0.009	17.831 ± 0.009	16.775 ± 0.003	15.429 ± 0.007
3	−7.023	175.32	17.536 ± 0.017	16.812 ± 0.014	16.450 ± 0.001	16.077 ± 0.002
4	−6.938	97.31	21.162 ± 0.020	19.709 ± 0.015	18.899 ± 0.006	18.090 ± 0.011
5	−3.270	−42.97	19.332 ± 0.007	18.822 ± 0.006	18.514 ± 0.008	18.189 ± 0.007
6	−1.733	172.50	15.598 ± 0.009	14.789 ± 0.020	14.373 ± 0.003	13.957 ± 0.001
7	0.000	0.00	16.472 ± 0.001	16.121 ± 0.001	15.904 ± 0.001	15.671 ± 0.001
8	5.302	−67.74	17.323 ± 0.016	16.697 ± 0.004	16.388 ± 0.014	16.034 ± 0.008

NOTE—Magnitudes have been derived with respect to the PSF template star (star 7). Reported error bars are from the observed dispersion between the images and do not include uncertainties in the magnitude of the reference star. *BVRI* uncertainties in the reference star's magnitude are ±0.007, ±0.011, ±0.014, and ±0.016 mag, respectively, and must be added in quadrature to the errors quoted above.

REFERENCES

Claeskens, J.-F., Surdej, J., & Remy, M. 1996, A&A, 305, L9
Geisler, D. 1996, AJ, 111, 480
Kochanek, C. S. 1996, ApJ, 466, 638
Kochanek, C. S., Falco, E. E., Impey, C. D., Lehár, J., McLeod, B. A., & Rix, H.-W. 1998, in AIP Conf. Proc. 470, After the Dark Ages: When Galaxies Were Young, ed. S. S. Holt & E. P. Smith (New York: AIP), 163
Kochanek, C. S., & Hewitt, J. N. 1996, Astrophysical Applications of Gravitational Lensing (Dordrecht: Kluwer)
Landolt, A. U. 1992, AJ, 104, 340
Maza, J., Wischnjewsky, M., Antezana, R., & González, L. E. 1995, Rev. Mexicana. Astron. Astrofis., 31, 119
Refsdal, S. 1964, MNRAS, 128, 307
Rosvick, J. M. 1995, MNRAS, 277, 1379
Schechter, P. L., Gregg, M. D., Becker, R. H., Helfand, D. J., & White, R. L. 1998, AJ, 115, 1371
Schechter, P. L., Mateo, M., & Saha, A. 1993, PASP, 105, 1342
Schechter, P. L., & Moore, C. B. 1993, AJ, 105, 1